Chemical Physics Letters 490 (2010) 245–248

Contents lists available at ScienceDirect

Chemical Physics Letters

journal homepage: www.elsevier.com/locate/cplett

Dissipative vibrational wave packet dynamics of alkali dimers attached to helium nanodroplets

Martin Schlesinger [a,*], Marcel Mudrich [b], Frank Stienkemeier [b], Walter T. Strunz [a]

[a] Institut für Theoretische Physik, Technische Universität Dresden, D-01062 Dresden, Germany
[b] Physikalisches Institut, Universität Freiburg, D-79104 Freiburg, Germany

ARTICLE INFO

Article history:
Received 22 January 2010
In final form 19 March 2010
Available online 24 March 2010

ABSTRACT

Femtosecond pump–probe spectroscopy has been used to study vibrational dynamics of potassium dimers attached to superfluid helium nanodroplets. Comparing the measured data with theoretical results based on dissipative quantum dynamics we propose that the most important effect of the helium environment is a general damping of the vibrational dynamics. The calculations allow us to explain crucial experimental findings that are unobserved in gas phase measurements. Remarkably, wave packet velocities of such alkali dimer vibrations are just about in the range of the Landau critical velocity of superfluid helium. We therefore also discuss a possible influence of superfluidity on the induced wave packet dynamics.

Helium (He) nanodroplets have become a useful matrix to study molecular species in an ultracold, weakly perturbing environment [1]. Consisting of 10^3—10^5 ^{4}He atoms, they provide a unique quantum solvent, which essentially isolates and effectively cools the impurity molecule of interest [2]. Spectroscopy of this ideally prepared molecular 'sample' provides insight into its interaction with the host [3], but also into the peculiar properties of the quantum matrix itself [4]. More specifically, characteristic features in the spectrum of embedded molecules are shifts and broadening of spectral lines, which allow studies of the influence of the surrounding He environment. Other features, such as the appearance of phonon wings in the spectra, may originate from the excitation of collective degrees of freedom of the droplet [5]. The droplets provide a versatile test bed for studying relaxation dynamics and cooling processes of immersed species [1,6]. In contrast to pure spectroscopic studies reported earlier, we here present time resolved femtosecond pump–probe measurements. This technique is well-established for studying vibrational wave packet (WP) dynamics of diatomic systems [7–11]. We investigate potassium molecules (K_2) attached to He nanodroplets (He nanodroplet isolation (HENDI) spectroscopy) [12]. The alkali dimers are not solvated, but found to reside on the surface of the droplet [5,13], as do alkali atoms [14].

The observed real time pump–probe spectra of K_2 on He droplets differ significantly from previously obtained gas phase results [12,15]. In this Letter, we argue that dissipative quantum dynamics, here employed through a quantum master equation, is crucial for the understanding of these measurements. Moreover, the dissipation has to be combined with stochastic desorption of the molecule and shifts of the potential energy surfaces induced by the He droplets to correctly describe the experimental results.

As we will elaborate at the very end of this manuscript, it so happens that the velocities of alkali dimer vibrations are of the order of Landau's critical velocity v_c in superfluid helium. Superfluidity manifests itself through the fascinating effect of frictionless flow below v_c [16]. In finite-sized quantum systems, superfluidity is a fundamental issue of current interest, both in liquid He [4,17,18] and in ultracold atomic gases [19]. Remarkably, we find best agreement with experimental findings when vibrational damping is omitted for very slowly moving WPs. This might hint at a direct influence of superfluidity and might show the potential of real time studies of vibrational motions to investigate the Landau critical velocity on the microscopic scale, very much in the spirit of vibrational wire resonators [20] or quartz tuning forks [21] that probe on larger scales.

In the pump–probe spectroscopy of K_2, potassium atoms are attached to He nanodroplets (~5000 atoms) which are created in a supersonic expansion of He gas at cryogenic conditions [12]. Doping conditions are chosen such that on average two potassium atoms stick to one droplet forming K_2 dimers which are weakly bound on the surface of the droplets. In a one color pump–probe excitation scheme the resulting K_2^+ photo ions are recorded mass selectively. A laser having 110 fs pulse width has been used providing 16 nJ pulses mildly focused in the interaction region with the molecular beam. The (3)-photon excitation schemes which are most relevant are depicted in Fig. 1.

The full numerical calculation of the pump–probe signal for dimers in the gas phase is detailed in Ref. [22] and only briefly outlined here. The dimer is described through the nuclear state vector

* Corresponding author.
E-mail address: Martin.Schlesinger@tu-dresden.de (M. Schlesinger).

0009-2614/$ - see front matter © 2010 Elsevier B.V. All rights reserved.
doi:10.1016/j.cplett.2010.03.060

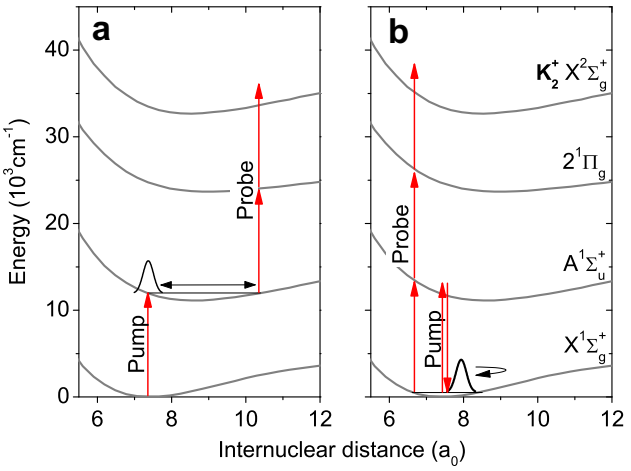

Fig. 1. Potential curves of the K_2 molecule and excitation schemes at $\lambda = 833$ nm (a) and at $\lambda = 800$ nm (b). The pump pulse creates vibrational WPs in various electronic states. Significant ionization through the probe pulse occurs in (a) only if a WP is located around the outer, and in (b) only if a wave packet is near the inner turning point (FC window).

$\Psi(t) = (\psi_X(t), \psi_A(t), \ldots)$. It contains a vibrational WP $\psi_i(t)$ in electronic state i after interaction with the pump pulse. The state vector of the isolated dimer obeys the time dependent Schrödinger equation (TDSE)

$$i\hbar\partial_t \Psi(t) = H\Psi(t). \tag{1}$$

The molecular Hamiltonian H is an $n \times n$ matrix, if n electronic states are taken into account. The diagonal elements of the matrix contain the kinetic energy and potential energy surface (PES), while off-diagonal elements contain the coupling induced by the interaction with the laser field. Transition dipole moments are assumed to be constant (Condon approximation). The split operator scheme allows to propagate the state vector numerically [23]. The fluorescence signal from a final state f is proportional to the occupation probability $|\psi_f(\tau)|^2$ after both pulses and depends only on the delay τ between pump- and probe pulse. Here, the final state consists of a (bound) molecular ion K_2^+ and an ejected electron with energy E_{e^-}. We use discretization of the (electronic) continuum, a technique successfully employed earlier [22]. The measured ion yield is proportional to the sum over all (discretized) electronic energies E_{e^-}.

Dimer dynamics on the droplet is altered by He-induced shifts of PES, which we take into account first. Systematic numerical tests reveal that best agreement with experiment is obtained when shifting the 2Π surface (by -50 cm^{-1}) which agrees well with findings in [12,24]. There is also a shift of the ionic surface [25]. However, as the excess energy of photo electrons is not observed here, the magnitude of this shift has no effect on our results.

Next, we take into account dimer desorption from the droplet at some random time t'; for $t > t'$ we set He-induced shifts to zero in the propagation scheme. The random desorption is modelled by assuming a constant desorption rate, leading to a probability density $P(t') \sim \exp\{-t'/\tau_D\}$ for the desorption time t' after electronic excitation.

We find that a description solely based on energy shift (parameter $\Delta_{2\Pi}$) and desorption (parameter τ_D) cannot reproduce crucial features of the HENDI measurements [26].

The new essential ingredient of our description is the inclusion of damping of vibrational WPs. Dissipation of vibrational energy occurs due to the interaction with collective degrees of freedom of the He droplets (phonons or ripplons). In our phenomenological approach we do not specify the microscopic dimer–droplet interaction. Instead, we use a well-established master equation, describing damping for near-harmonic systems at effectively zero temperature fully quantum mechanically (see [27]). Thus, the dynamics of the full vibrational density operator ρ is determined from

$$\dot{\rho} = -\frac{i}{\hbar}[H, \rho] + \frac{1}{2}\sum_i \gamma_i (2a_i \rho a_i^\dagger - a_i^\dagger a_i \rho - \rho a_i^\dagger a_i). \tag{2}$$

Here, H denotes the molecular Hamiltonian from Eq. (1) and $a_i, a_i^\dagger$ are the annihilation/creation operators obtained from a harmonic approximation of the PES corresponding to electronic state i. For numerical purposes, the equation for the mixed state, Eq. (2), is replaced by a (stochastic) differential equation for a state vector ('quantum state diffusion', see, e.g. [28]) which allows us here to stick with the split operator propagation method. In order to recover the density operator ρ, one has to average over several realizations.

We choose the parameters for damping (rates $\gamma_i \equiv \gamma$) and desorption (time τ_D) to be state-independent. Note, however, a possible influence of the orientation of the dimer on damping dynamics as discussed for Li_2 in [29]. We here assume no change of alignment during dynamics.

Excitation at a wavelength of 833 nm almost exclusively follows the path sketched in Fig. 1a and probes the WP propagation in the $A^1\Sigma_u^+$ electronic state [11]. The probe pulse leads to an enhanced population of the final ionic state only if the WP is located at the outer turning point, where the intermediate 2Π state opens a Franck–Condon (FC) window. The resulting oscillatory structure (Fig. 2) in the ion rate reflects the dynamics of the WP in the A state. The simulation of the ion signal for the gas phase is shown in Fig. 2b and agrees with earlier gas phase results [9]. The weak overall decrease of the oscillation amplitude in Fig. 2b is caused by the spreading of the initially well-localized WP in the anharmonic potential. This gas phase result is markedly different from the experimental HENDI spectrum (Fig. 2a), which is a clear sign of the effect of the He environment. The measured signal shows an exponential decay of the initial amplitude which is well captured by our calculations (Fig. 2c). The persisting oscillations are also reproduced, yet with a smaller amplitude.

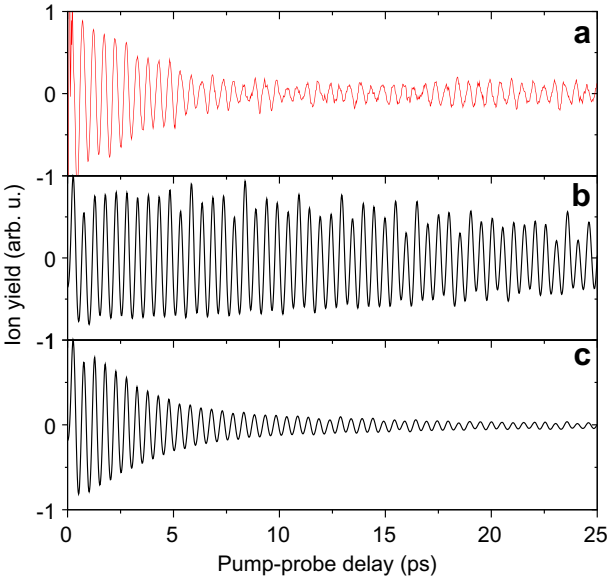

Fig. 2. Pump–probe signal for $\lambda = 833$ nm. (a) Experimental HENDI result (from Ref. [12]). (b) Numerical simulation for the gas phase (see also [9]). (c) Calculated signal assuming He-induced damping, shift of PES and desorption of the molecule.

Best agreement between experiment and our theory is obtained when damping, shift and desorption are included into the calculation with parameters $\gamma = 0.15/\text{ps}$, $\Delta_{2\Pi} = -50\ \text{cm}^{-1}$ and $\tau_D = 8$ ps (Fig. 2c). The dependence of all our findings on these precise values is rather smooth and only after leaving a $\pm 5\%$ interval significant deviations from the displayed figures occur.

It is tempting to relate the damping rate γ to measurements of the viscosity η in liquid He (see [21]). However, such values for η are based on macroscopic theories which are not applicable here. Note that in [29] the authors investigate dissipative alkali dimer dynamics on a microscopic scale by studying collisions with ^{4}He atoms. Remarkably, the calculated friction coefficient for singlet systems (0.06/ps) turns out to be of the order of magnitude of our γ.

The temporal evolution and intensity of certain frequency components can be visualized by employing sliding window Fourier transforms (FT) on the time-dependent signal (giving the spectrogram $S(\omega, \tau)$ [10]). Here we choose a 3 ps time window. As discussed in Ref. [12], in the experiment at 833 nm excitation wavelength a small increase of the frequency of the WP motion during the first 10 ps is observed. In Fig. 3 this behavior (if less pronounced) is seen in the FT spectrum of our calculated signal, provided damping is included. The findings allow the following interpretation: during the first few picoseconds the contribution of the damped molecules is most important. As a consequence of the anharmonic potential, they vibrate with a higher frequency, explaining the initial shift of the main frequency $\omega_A^{833\ \text{nm}}$ to slightly larger values (or lower vibrational quantum numbers). Later on, for times $\tau > 10$ ps, vibrationally damped molecules no longer contribute, as a closing of their FC window takes place. Hence, only molecules which desorb very early and thus do not suffer vibrational damping contribute to the ion yield at late delay times. Consequently, a weak oscillatory signal persists in the time domain and in the windowed FT the main frequency returns to the original gas phase value.

At the shorter wavelength $\lambda = 800$ nm the excitation scheme sketched in Fig. 1b applies. Here, a WP in the ground state, excited through stimulated Raman scattering (RISRS), can be visualized through 3-photon absorption. In the gas phase, this process is superposed coherently with transitions from higher lying electronic states near their respective inner turning points, leading to interferences in the ionic state. A more detailed analysis shows that in the gas phase the interference is indeed destructive: the contribution of the WP on the X surface is missing in the gas phase (see Fig. 4b) – similar findings were reported in Ref. [30]. Without any damping mechanism, contributions from the A state (component $\omega_A^{800\ \text{nm}} \approx 64\ \text{cm}^{-1}$) and from the 2Π state (component $2\,\omega_{2\Pi}^{800\ \text{nm}} \approx 86\ \text{cm}^{-1}$) are dominant, which is not observed in the

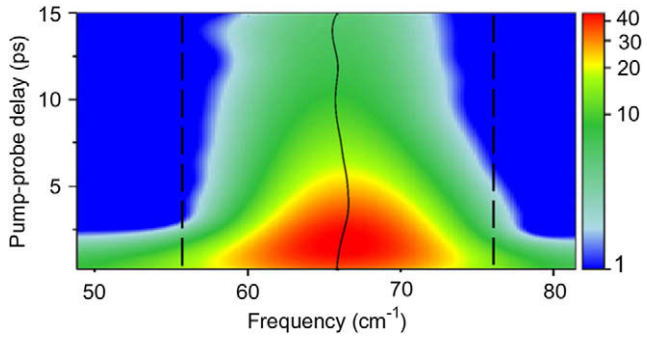

Fig. 3. Calculated spectrogram $S(\omega, \tau)$ for $\lambda = 833$ nm. The dominant frequency is slightly shifted to larger values for short delay times (the black solid line indicates the mean frequency between the dashed lines as a function of time).

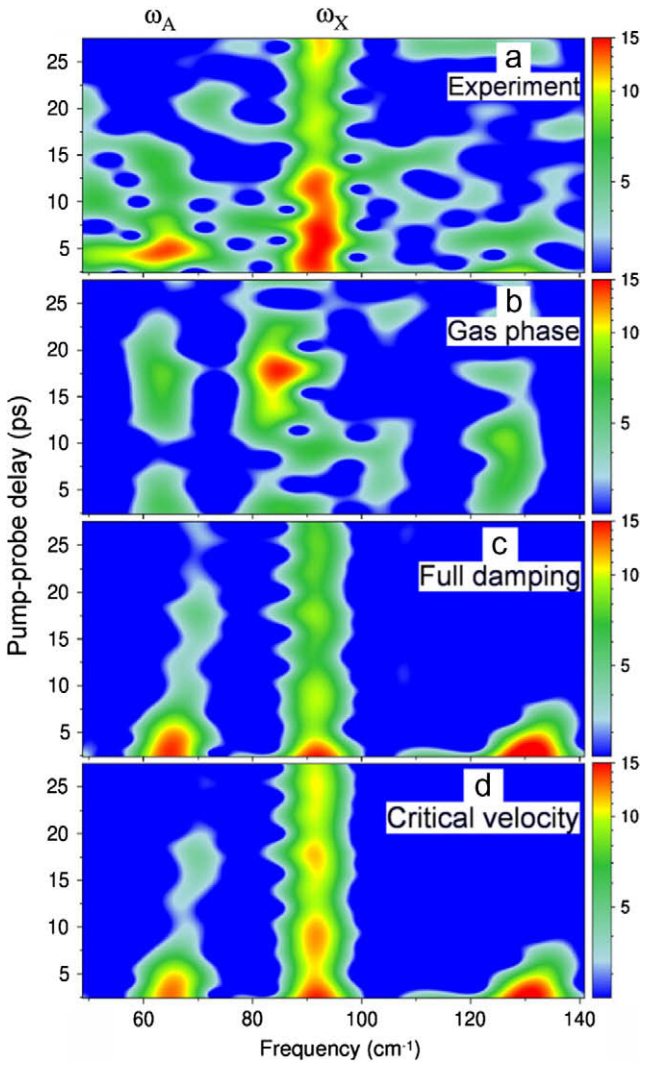

Fig. 4. Spectrograms $S(\omega, \tau)$ showing the WP dynamics at $\lambda = 800$ nm for the experimental HENDI result (a), for the gas-phase simulation (b), for the fully damped model (c), and for a model including a critical velocity (d) (see text).

He droplet experiment (Fig. 4a). There, although $\omega_A^{800\ \text{nm}}$ is present during the first 5 ps, it fades out and only the component $\omega_X^{800\ \text{nm}} \approx 91\ \text{cm}^{-1}$ (WP in X state) contributes at later delay times. We now include damping for $\lambda = 800$ nm with precisely the same parameters as for the considerations at $\lambda = 833$ nm. The corresponding spectrogram $S(\omega, \tau)$ (Fig. 4c) agrees remarkably well with experimental findings in many respects. The component at $\omega_A^{800\ \text{nm}}$ fades out after several ps due to vibrational damping: the WP in the A state leaves the initial FC window at the inner turning point.

More significant is the behavior of the component near $\omega_X^{800\ \text{nm}}$, ascribed to the ground state WP. It is clearly visible in the experimental and theoretical (including damping) spectrogram, yet absent in the gas phase. Damping of the WPs in the A and 2Π state enhances ionization from the ground state by the probe pulse, since the mapping of the X state dynamics to the ion no longer suffers from destructive interference with competing processes near the inner turning point on the A and 2Π surfaces. Once again we see a nice agreement between experimental findings of dimer dynamics on the He droplet and theoretical modelling based on dissipative quantum dynamics.

Yet, there is an even more intriguing observation: the results at 800 nm might hint at a direct influence of superfluidity on these

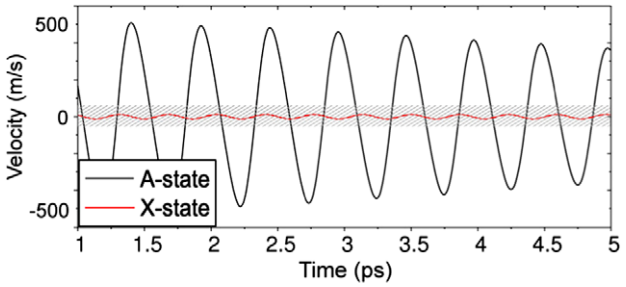

Fig. 5. Dynamics in velocity domain of a WP excited in the electronically excited A-state and in the ground state X. The hatched area indicates velocities below the critical value of 60 m/s.

spectra. Particles may move unhindered through a superfluid as long as their velocity does not exceed the (Landau) critical velocity v_c [16].

Recall that the wave packets describe the relative motion of atoms within the molecule: in a simple approach we determine the corresponding atomic velocity relative to the He droplet from the average velocity $\langle v\rangle = \langle\widehat{P}\rangle/2\mu$ of the nuclear WP. Once it drops below the critical velocity (we chose the bulk value $v_c = 60$ m/s), we set the friction coefficient to zero (see also [31]) and compare with the fully damped model. For the excitation at $\lambda = 833$ nm, it is the dynamics on the A surface that dominates the observations. This vibration, however, is fast and the corresponding velocity oscillates between ±500 m/s (see Fig. 5). For most of the time, therefore, friction is present and the influence of v_c is hardly noticeable. For an excitation at wavelength $\lambda = 800$ nm, however, the motion on the X surface is so slow (at most $v \approx 15$ m/s, see Fig. 5) that it is tempting to simply neglect damping on that surface entirely ($\gamma_X = 0$).

The resulting spectrogram (Fig. 4d) shows that the component $\omega_X^{800\text{ nm}}$ is even more pronounced compared to the previous calculation (full damping, Fig. 4c) and agreement with experiment (Fig. 4a) is even better.

In conclusion, the study of vibrational wave packets in dimers attached to He nanodroplets exhibits clear deviations from previous gas phase results. A model based on shifts of potential energy surfaces, desorption from the host and, most importantly, damping of the wave packets is able to explain crucial features of the measurement. For excitation at $\lambda = 833$ nm the decay of the signal and a small shift in the FT spectrum are reproduced. Damping of excited state wave packets enhances the mapping of the ground state dynamics to the ion signal, as realized at $\lambda = 800$ nm.

Most remarkably, in our studies best agreement with experiment is obtained when we neglect damping for very slowly moving wave packets. This observation might be attributed to the role of the critical velocity in these experiments, which turns out to be larger than the velocity of the motion on the X surface. For finite systems like droplets, due to the influence of size, density, geometry etc., a value of v_c different from the bulk value (~60 m/s) is likely. This, however, is not expected to change the essentials of our arguments as long as v_c is larger than some 20 m/s. Thus, the influence of superfluidity might be directly visible, opening the door for further interesting studies: choosing heavier molecules for which the vibrational velocities are well below some 100 m/s might enable us to investigate friction and frictionless motion on the atomic scale.

We stress that in view of the good agreement between experiment and our results, it appears that the complex molecule–droplet interaction may effectively be described by a few parameters. Thus, it is certainly desirable to derive γ, Δ or τ_D from a microscopic approach. Then we should be able to relate these parameters to properties of the He droplet surface (e.g. spectrum of elementary excitations) and to more details of the molecule–droplet interaction (dependence on molecular orientation, for instance). We strongly believe that further studies with attached probe molecules, such as current investigations with alkali spin triplet systems [32], will help to get a deeper understanding of surface properties of helium nanodroplets.

Acknowledgements

We thank Jan Handt and Ralf Schützhold for stimulating discussions and C.P. Schulz for experimental aid. We also thank the unknown referees for their beneficial reports. Support by the Deutsche Forschungsgemeinschaft (DFG) is gratefully acknowledged. Computing resources have been provided by the Zentrum für Informationsdienste und Hochleistungsrechnen (ZIH) at the TU Dresden. M. Schlesinger is a member of the IMPRS Dresden.

References

[1] J.P. Toennies, A.F. Vilesov, Angew. Chem. 43 (2004) 2622.
[2] M. Hartmann, R.E. Miller, J.P. Toennies, A. Vilesov, Phys. Rev. Lett. 75 (1995) 1566.
[3] Y. Kwon, P. Huang, M.V. Patel, D. Blume, K.B. Whaley, J. Chem. Phys. 113 (2000) 6469.
[4] M. Hartmann, F. Mielke, J.P. Toennies, A.F. Vilesov, G. Benedek, Phys. Rev. Lett. 76 (1996) 4560.
[5] F. Stienkemeier, J. Higgins, W.E. Ernst, G. Scoles, Phys. Rev. Lett. 74 (1995) 3592.
[6] F. Stienkemeier, K.K. Lehmann, J. Phys. B: At. Mol. Opt. Phys. 39 (2006) 127.
[7] R. Bowman, M. Dantus, A. Zewail, Chem. Phys. Lett. 161 (1989) 297.
[8] T. Baumert, V. Engel, C. Röttgermann, W.T. Strunz, G. Gerber, Chem. Phys. Lett. 191 (1992) 639.
[9] R. de Vivie-Riedle et al., J. Phys. Chem. 100 (1996) 7789.
[10] S. Rutz, E. Schreiber, Chem. Phys. Lett. 25 (1997) 9.
[11] C. Nicole, M.A. Bouchene, C. Meier, S. Magnier, E. Schreiber, B. Girard, J. Chem. Phys. 111 (1999) 7857.
[12] P. Claas, G. Droppelmann, C.P. Schulz, M. Mudrich, F. Stienkemeier, J. Phys. B: At. Mol. Opt. Phys. 39 (2006) S1151.
[13] F. Ancilotto, G. DeToffol, F. Toigo, Phys. Rev. B 52 (1995) 16125.
[14] F. Dalfovo, Z. Phys. D: At. Mol. Clusters 29 (1994) 61.
[15] K. Nauta, R.E. Miller, J. Chem. Phys. 113 (2000) 9466.
[16] L. Landau, J. Phys.: USSR 5 (1941) 71.
[17] S. Grebenev, J.P. Toennies, A.F. Vilesov, Science 279 (1998) 2083.
[18] J. Tang, Y.J. Xu, A.R.W. McKellar, W. Jäger, Science 297 (2002) 2030.
[19] J.R. Anglin, W. Ketterle, Nature 416 (2002) 211.
[20] A. Kraus, A. Erbe, R.H. Blick, Nanotechnology 11 (2000) 165; C.A.M. Castelijns, K.F. Coates, A.M. Guenault, S.G. Mussett, G.R. Pickett, Phys. Rev. Lett. 56 (1986) 69.
[21] A.A. Zadorozhko, E.Y. Rudavskii, V.K. Chagovets, G.A. Sheshin, Y.A. Kitsenko, Low Temp. Phys. 35 (2009) 100.
[22] R. de Vivie-Riedle, B. Reischl, S. Rutz, E. Schreiber, J. Phys. Chem. 99 (1995) 16829.
[23] M. Feit, F. Fleck, A. Steiger, J. Comput. Phys. 47 (1982) 412.
[24] P. Claas, Ph.D. Thesis, Fakultät für Physik, Universität Bielefeld, 2006.
[25] E. Loginov, D. Rossi, M. Drabbels, Phys. Rev. Lett. 95 (2005) 163401.
[26] M. Schlesinger, W.T. Strunz, in preparation.
[27] M.O. Scully, M.S. Zubairy, Quantum Optics, Cambridge University Press, 1997.
[28] I.C. Percival, Quantum State Diffusion, Cambridge University Press, 1998.
[29] S. Bovino, E. Coccia, E. Bodo, D. Lopez-Duran, F.A. Gianturco, J. Chem. Phys. 130 (2009) 224903.
[30] T. Baumert, V. Engel, C. Meier, G. Gerber, Chem. Phys. Lett. 200 (1992) 488.
[31] D. Bonhommeau, A. Viel, N. Halberstadt, J. Chem. Phys. 120 (2004) 11359.
[32] M. Mudrich, P. Heister, T. Hippler, C. Giese, O. Dulieu, F. Stienkemeier, Phys. Rev. A 80 (2009) 042512.